ELSEVIER

Carbohydrate Polymers 37 (1998) 49–60

Carbohydrate Polymers

# Investigation of the physical network of amorphous amylose by slow calorimetry

P. Le Lay*, G. Delmas

*Université du Québec à Montréal, Département de chimie, CP 888, Succ. Centre-Ville, Montréal, Québec, Canada H3C 3P8*

Received 28 June 1997; revised 5 December 1997; accepted 8 December 1997

**Abstract**

To understand the origin of the temperature stability of amorphous amylose, we have investigated its interaction with water. Three calorimetric techniques, DSC in a slow temperature ramp (T-ramp) ($v = 1–6$ K/h) and isothermal calorimetry were used. They show that the network phase can be disordered when temperature ($T$) increases. The enthalpy of disordering reaches 60 J/g at $v = 1$ K/h but is lower for faster T-ramps. This newly found enthalpy modifies the calorimetric evaluations of order, which now approaches the spectroscopic value. We suggest that the stability of the network phase of amylose, i.e. the delay in the phase change from order to disorder is due to strain on the network chains generated by solvent expansion during the T-ramp. Phase transition by DSC is possible only when heating conditions avoid strain build-up in the sample. The little-known concepts of the effect of strain on a phase-change and of strain building in a network offer strategies to control the fraction of amylose which is resistant to enzyme attack. The fraction is associated with the network fraction. Non-crystalline amylose is found to contain about equal quantities of network and amorphous phases. 

*Keywords:* Amylose; Water; Heat; Physical network; Strained dissolution; Enzyme-resistant; Polyolefins

## 1. Introduction

Amylose is predominantly a linear polymer of (1 → 4)-α-D-glucan chains. It is one of the components of starch, the main one being amylopectin, a polysaccharide similar to amylose but containing branches in the 6-position. Amylose can be extracted from starch by many means, for example through the formation of a water-insoluble complex with 1-butanol. Due to inter- and intra-chain hydrogen bonds between the chains, a range of organizations or of orders can be found in amylose samples (Gidley et al., 1995; Appelqvist et al., 1993; Welsh et al., 1992; Cooke et al., 1992; Gidley et al., 1989; Gidley and Bociek, 1985).

### *1.1. Amylose/water mixtures*

Most of the amorphous amylose samples contain two ''entangled'' fractions, a fraction which swells in water at room temperature (RT) and another which is insoluble. The insoluble fraction changes gradually with increasing temperature so that a transparent solution can be obtained. In a dilute solution which has undergone a high temperature treatment, the solubility of amylose and the stability of the solution are sufficient to allow viscosity or light scattering measurements. The conformation of amylose molecules is found to be a random coil in water (Banks et al., 1975; Miles et al., 1985a). The dilute solutions are not infinitely stable. Different techniques such as turbidity (Clark et al., 1989; Miles et al., 1985b), modulus (Welsh et al., 1992; Clark et al., 1989; Miles et al., 1985a, b), viscosity (Banks et al., 1975), $^{13}C$ NMR analysis (Dev et al., 1987; Gidley and Bociek, 1985), swelling (Hollinger et al., 1974), change of volume (Miles et al., 1985a), X-ray scattering (Cooke et al., 1992; Miles et al., 1985a, b) can be used to follow the spontaneous growth with time of different kinds of order; namely, the long-range order, the short-range order and the order present in the network phase. The network phase gives to the mixture the gelling properties. It consists of chains linked by junctions of different nature (small crystals, entanglements, hydrogen bonds). Alternatively, the loss of order of amylose suspensions in water when $T$ increases can be investigated with the same techniques. Calorimetric analysis has been used extensively for determining the amount of long-range order lost with temperature increase (Noël et al., 1992; Hollinger et al., 1974; Durrani et al., 1995; Sievert et al., 1993a, b) by water/amylose mixtures

* Corresponding author

0144–8617/98/$ - see front matter 
*PII* S0144-8617(97)00257-9

with different histories. Much less data have been obtained for the evaluation of short-range order loss for reasons which will be explained below. The term short-range order will be used here for order which does not contribute to sharp X-ray diffraction peaks. Several papers of Gidley's group have reported that the fraction of order found by quantitative $^{13}C$ NMR is generally higher than that by X-ray diffraction.

### *1.2. Features of a dissolution trace in the presence of a network*

The dissolution traces of crystalline amylose samples as followed by thermal analysis show an endotherm of ''dissolution'' at $T_d$ (around 70°C). The X-ray diffraction pattern of the material becomes flat above $T_d$. This temperature corresponds to the disappearance of long-range order. In the case of starch samples, $T_d$ corresponds to the gelatinization, i.e. the disruption of the starch granules in water and also to the disappearance of long-range order. The endotherm of gelatinization is not seen in amylose samples which have a flat X-ray pattern. Above $T_d$, the starch/water or amylose/water mixtures are not homogeneous solutions. The suspensions stay somewhat turbid up to high temperatures, possibly 50–70 K above $T_d$. A residual organization in the mixture above $T_d$ explains the usual practice of raising amylose/water mixtures to a high temperature, $T_{max}$ (with $120 < T_{max} < 150$°C) to recover a homogeneous system on cooling. However, the loss of that residual organization has not been observed by DSC. Observation by light microscopy of some autoclaved preparations show birefringent regions associated with non-gelatinized fractions in the sample. This means that the homogeneity of the sample after the high-temperature treatment is not total. Isolation of the non-gelatinized fraction is a method of preparation of enzyme resistant amylose.

### *1.3. Case of polyolefins*

Melts of polyolefins have some features in common with solutions of amylose at high temperature. They show regions of birefringence which disappear very slowly with time when the melt (or the solution) is left above $T_m$, the melting temperature of long-range order (or of $T_d$). This heterogeneity of the melt is further confirmed by the observation of two relaxation times in $^{13}C$ NMR. Recent analysis of the melting and dissolution processes of polyolefins by slow calorimetry has led to the understanding of the origin of the birefringence in the melt and of peculiar features of their solutions (Phuong-Nguyen et al., 1992a, b, 1994a–c; Doublier et al., 1992; Morin et al., 1995). A new phase, a network phase of short-range order, has been found. The order of the network phase raises the value of order found in gels by calorimetry to that obtained by spectroscopy. The main features of slow calorimetry will be presented in the discussion.

We suggest that a network phase is also present in amylose. The aim of the present investigation is to verify this hypothesis and characterize the network phase of amylose by calorimetry. We will present calorimetry in a slow T-ramp on amylose suspensions and isothermal calorimetry (i.e. heats of interaction between water and dry amylose at a given temperature).

## 2. Materials and methods

### *2.1. Materials*

Potato amylose, type III, essentially free of amylopectin was obtained from Sigma Chemical Co. (St. Louis, MO). Glucose was purchased from the Aldrich Co. (Milwaukee, WI). Distilled water was been used as solvent.

A small amount of the as-received amylose was left at RT, 2–3 days in a dessicator, with an excess of $P_20_5$ drying agent, to be thoroughly dried before experiments.

### *2.2. Methods*

#### *2.2.1. Calorimeters and procedures*

We used a Perkin Elmer differential scanning calorimeter DSC7 for the measurement of the heat of fusion of glucose. The ramp was programmed from 50 to 180°C at 5°C/min. We found a heat of 180 J/g.

For amylose studies, three series of measurements are reported, (A)–(C) which were obtained with a Setaram calorimeter in a T-ramp (A), with a Hart calorimeter (B), and both in a slow T-ramp and with a Setaram calorimeter in an isothermal mode (C).

Before describing the calorimeter measurements, it should be pointed out that isothermal measurements and those in a slow T-ramp have a different quality requirement. Due to the relatively short duration of an isothermal mode experiment, the long-term stability of the calorimeter is not essential. On the other hand, integration of small heat flow requires an accurate and very stable baseline. Comparison of data from different calorimeters working at an isothermal mode are straightforward; but the comparisons of data obtained by two calorimeters programmed in a slow T-ramp and having a different stability may be risky. In the C80 calorimeter the large size of the heat block assures a stable baseline, a feature not reached in a calorimeter in which the volume of the heat block reaches only a few cubic centimeters.

A: Setaram calorimeter in a slow T-ramp (40–140°C)

The calorimeter was a differential calorimeter (Seteram, Lyon, France) the large stainless steel cells of which (OD = 16 mm, height = 95 mm) allow for solution work. It was used extensively in our group for the investigation of phase-changes in polyolefins and their gels and solutions. Its stability and sensitivity are

such that the small heat flows which are produced in slow T-ramps can be measured accurately. It was this accuracy which was crucial in the polyolefin work, i.e. in the discovery of phase-changes with slow kinetics (Phuong-Nguyen et al., 1994a, b). The enthalpy changes in this paper have been obtained with a T-ramp of 1, 3 and 6 K/h. At 3–6 K/h the background noise is about 5 $\mu$W and at 1 K/h it is lower.

The sample was not placed directly in the cell but in a glass tube which was subsequently sealed and introduced in the cell. This had the advantage of avoiding solvent evaporation and degradation and of leaving the sample ready for re-run after different cooling processes, aging and retrogradation. The reference cell was made with the same heat capacity as the sample cell.

Procedure: a known weight of dried amylose was stirred in an excess of water for 3 h. The suspension was centrifuged at low speed for 10 min. The concentration of amylose in the centrifuge pellet (about 3 $cm^3$) obtained by weighting was between 13 and 17%. The pellet was then placed in the glass tube. The latter was sealed and introduced into the calorimeter.

Baseline: the slight inbalance of the two sides of the calorimeter led to a slanted signal before baseline subtraction. The slope of the signal increased with the rate of heating and the temperature. As in recent work (Phuong-Nguyen et al., 1995) the baseline has been subtracted in the traces given below.

B: Hart calorimeter in a slow T-ramp (5–90°C)

Measurements were made with a Hart 7707 differential heat conduction scanning calorimeter equipped with three cells. They were filled with 0.5–0.8 $cm^3$ of the sample which had been submitted to the same procedure as in (A). The initial temperature was either 5 or 15°C. After a 3–4 h equilibrium time, the T-ramp was started up to 98°C. In most of the experiments, particularly those with the fastest T-ramp, one of the cells was filled with water. The baseline obtained with water alone was subtracted using a program supplied by the company. The Hart calorimeter was more sensitive than the Setaram calorimeter but less stable. Its maximum working temperature (100°C) was a limitation for the measurements presented here.

C: Setaram calorimeter in an isothermal mode (heats of swelling)

Isothermal measurements of interaction between amylose and water and glucose and water were carried out in the Setaram calorimeter using breakable cells. A known weight of dried amylose (about 20 mg) was placed in a home-made thin glass bulb and sealed under vacuum. The bulb was placed with water in a cell equiped with Teflon joints to prevent water evaporation and then the cell was placed in the calorimeter. After thermal equilibrium, the bulb was broken by pushing gently from the top of the calorimeter a stem going through the stopper of the cell. Due to the vacuum in the bulb, water filled the entire glass bulb once it was broken and interacted with amylose or glucose. A sharp signal (Fig. 3) was obtained which returns to the baseline in less than 2 h. Without vacuum in the bulb, wetting was not complete, the swollen amylose preventing water entering the bulb and wetting the entire material.

The experimental heats obtained after integration of the heat flow change were, for (C), the sum of three contributions:

$$\Delta H_{(\text{experimental})} = \Delta H_{\text{interaction}} + \Delta H_{\text{glass-breaking}} + \Delta H_{\text{vaporization}} \quad (1)$$

$\Delta H_{\text{glass-breaking}}$ obtained without water was about $-200$ mJ and $\Delta H_{\text{vaporization}}$ depended on the temperature. It corresponded to the endothermic heat of vaporization of water in the volume of the bulb which was not saturated by water vapor. $\Delta H_{\text{vaporization}}$ could be calculated from the volume of the bulb and the equilibrium water pressure at a given temperature. Alternatively, the heat of a blank experiment could be used to measure the second and third term of Eq. (1). This heat, subtracted to $\Delta H_{(\text{experimental})}$ to obtain $\Delta H_{\text{interaction}}$, varied between $-150$ mJ at 25°C and 500 mJ at 80°C. The data given in Table 2 are $\Delta H_{\text{interaction, specific}}$ obtained by dividing $\Delta H_{\text{interaction}}$ by the weight of dry amylose.

The calculated values of $\Delta H_{\text{vaporization}}$ are systematically larger than the experimental ones. The difference can reach 20% at high temperature. This signifies that the actual volume of vacuum is smaller than that of the bulb. It is likely that a small quantity of air at the temperature of the calorimeter enters the cell through the stem orifice during the aspiration caused by the breaking of the evacuated glass bulb.

The calibration constant of the calorimeter is obtained by the Joule effect. Using the measured constant, the value of $\Delta H_{\text{interaction, specific}}$ for glucose is within 1% of the published value (Jasra et al., 1982).

### 2.3. Contribution to the heat effects

The non-crystalline amylose is assumed to be composed of two phases, the amorphous phase which interacts with water with an exothermic heat ($\Delta H_{\text{H-bonding}}$), and the network phase which can be disordered with an endothermic heat ($\Delta H_{\text{disor.network}}$). The fractions of these two phases are respectively $\alpha_a$ and $1 - \alpha_a$. Using this simple two-phases model the total heat effect can be written in terms of the composition of the material, for any temperature and per gram, as:

$$\Delta H_{\text{interaction, specific}}(T) = \alpha_a \Delta H_{\text{H-bonding, specific}}(T) + (1-\alpha_a) F \Delta H_{\text{disor.network, specific}}(T) \quad (2)$$

where $\Delta H_{\text{H-bonding,specific}}$ and $\Delta H_{\text{disor.network,specific}}$ are the heats

associated, respectively, with interactions with water of the completely amorphous amylose and the amylose network phase, and $F$ is the fraction of network which has been disordered at the temperature $T$. It is assumed that the network phase does not contribute to $\Delta H_{\text{H-bonding}}$.[1]

### 2.4. Measurement of $\alpha_a$ through data on a model molecule, glucose

Glucose is a crystalline molecule which dissolves in water with a large endothermic heat. It contains the heat of fusion which can be measured directly on the dry sample and is equal to 180 J/g. By subtracting the heat of fusion from the heat of immersion, one obtains the heat of interaction of amorphous glucose with water.

Since glucose is completely soluble in water, its molecules can be assumed to behave, when solubilised in water, like the amorphous phase of amylose. This comes from the assumption ($\alpha_a = 1$) that the second term of the right-hand side of Eq. (2) is zero. Furthermore, the specific interaction with water of the small molecule and of the polymer are similar. For this model molecule the experimental value of the heat of immersion gives:

$$\Delta H_{\text{interaction, specific}}(\text{glucose})(25^\circ\text{C}) = \Delta H_{\text{H-bonding, specific}}(25^\circ\text{C}) \quad (3)$$

Eq. (2) can be simplified if it is assumed that the dissolution of the network is negligible at 25°C, i.e. $F = 0$ at 25°C:

$$\Delta H_{\text{interaction, specific}}(\text{amylose})(25^\circ\text{C}) = \alpha_a \Delta H_{\text{H-bonding, specific}}(25^\circ\text{C}) \quad (4)$$

Comparison of Eqs. (3) and (4) gives $\alpha_a$ assuming that the values of $\Delta H_{\text{H-bonding,specific}}$ are the same for the polymer and the model molecule:

$$\alpha_a = \Delta H_{\text{interaction, specific}}(\text{amylose})(25^\circ\text{C}) / \Delta H_{\text{interaction, specific}}(\text{glucose})(25^\circ\text{C}) \quad (5)$$

### 2.5. Measurement of $\Delta H_{\text{disor.network,specific}}$ in a T-ramp

In the case of the T-ramp, the first term of the right-hand side of Eq. (2) represents an interaction that occurs during suspension of the sample in water, prior to placing the sample in the calorimeter. So the heat effect is written as:

$$\Delta H_{\text{interaction, specific}}(T) = (1 - \alpha_a) \times F \times \Delta H_{\text{disor.network, specific}}(T) \quad (6)$$

The integration of the signal (i.e. of the solution heat capacity between $T_{\text{initial}}$ and $T_{\text{final}}$) gives directly the right-side of Eq. (6). If $\alpha_a$ and $\Delta H_{\text{disor.network,specific}}$ are known, the value of $F$ is obtained.

### 2.6. Measurement of $\Delta H_{\text{disor.network,specific}}$ through isothermal data

In the case of an isothermal measurement of the heat of immersion, Eq. (2) is used. To find the value of the second term at a given temperature, the values of $\alpha_a$ and $\Delta H_{\text{H-bonding,specific}}(T)$ have to be known. $\alpha_a$ is obtained as outlined above and the variation of $\Delta H_{\text{H-bonding,specific}}(T)$ is obtained through data on glucose using assumptions of our model:

$$\Delta H_{\text{interaction, specific}}(\text{glucose})(T) = \Delta H_{\text{H-bonding, specific}}(T) \quad (7)$$

The enthalpy of disordering the network as $T$ increases will be obtained by finding the difference between the value of $\Delta H_{\text{interaction,specific}}(T)$ and that corresponding to the heat coming from the amorphous phase. Since amylose has a fraction $\alpha_a$ of amorphous phase, the value of the heat obtained on glucose (Eq. (7)) will be multiplied by $\alpha_a$ for the subtraction:

$$\Delta H_{\text{disor.network, specific}}(T) = (\text{Eq. 3})(T) - \alpha_a \times (\text{Eq. 7}(T)) \quad (8)$$

The experimental heats of immersion for amylose and glucose are used to calculate the difference.

### 2.7. The enthalpy of total network disordering

#### 2.7.1. $\Delta H_{\text{disor.network,specific}}$ (max.)

The integration of the network endotherms, over the 30–140°C interval, in technique (A) gives a value of the heat of disordering (right-hand side of Eq. (6)) which reflects the amount of disorder created in the network in the actual experiment. To evaluate the choice of the conditions of melting/dissolution and $\alpha_a$, it would be useful to know the maximum value of $\Delta H_{\text{disor.network,specific}}$, i.e. $\Delta H_{\text{disor.network,specific}}$ (max.). The fraction $F$ of order melted is:

$$F = \Delta H_{\text{disor.network, specific}} / \Delta H_{\text{disor.network, specific}}(\text{max.}) \quad (9)$$

Low and high values of $F$ are found respectively for conditions of dissolution which lead to respectively high and low strain. At this point it may be worthwhile to add information obtained for other chain molecules which have, as amylose does, a network phase. For polyolefins, the enthalpy of fusion of perfect crystals has been obtained previously through model molecules or other techniques. It is 293 J/g for linear polyethylene (PE). If a sample has 50% of

[1] Justification of a two-phase description of the amorphous amylose related to the magnitude of its interaction with water is based on molecular modeling and thermodynamic study (Fringant et al., 1995; Neregin et al., 1986). However, the crystalline phase is also reported to interact with water (Strauss et al., 1990) but to a lesser extent. One does not know the extent of the interaction with water of the network phase. Its temperature stability in the presence of water, greater than that of the long-range order phase, is an indication that it is the phase which interacts the less with water. Accordingly, the two-phase model of Eq. (2) based on the magnitude of the interaction with water will be left as a useful description of the amorphous phase.

Table 1
Values of $\Delta H_{\text{disor.network,specific}}$ by DSC

| | Setaram calorimeter (30–140°C) | | | Hart calorimeter (5–98°C) | | |
|---|---|---|---|---|---|---|
| T-ramp (K/h) | 1 | 3 | 6 | 1 | 3 | 30 |
| $\Delta H_{\text{disor.network,specific}}$ (J/g) | 60 | 26[a] | 12[a] | 20–30[a,b] | 8–15[a,b] | 5–7[a,b] |

[a] In the conditions of the measurements, the disordering is not complete.
[b] Uncertainty in the value of $\Delta H_{\text{disor.network,specific}}$ is due to the insufficient stability of the baseline.

long-range order, the endotherm of melting by fast DSC (the main peak of Fig. 6) has an enthalpy of fusion of about 150 J/g. We have found (Phuong-Nguyen et al., 1992a, b) for PE and isopolypropylene (iPP) (Phuong-Nguyen et al., 1995) that $\Delta H_{\text{disor.network,specific}}$ (max.), as measured experimentally has a magnitude similar to that of the long-range order when the disordering is complete.[2] For that particular sample of PE, the maximum value of $\Delta H_{\text{disor.network,specific}}$ i.e. $\Delta H_{\text{disor.network,specific}}$ (max.) will be found to be 150 J/g (i.e. $0.5 \times 293$ J/g).

### 2.8. Case of amylose

By the same argument as above an upper limit of $\Delta H_{\text{du.l6zh}}$ (max.) can be estimated through the heat of fusion of our model molecule, glucose, which is 180 J/g. Using this value with $\alpha_a = 0.47$ (see the calculation of $\alpha_a$ below) and $F = 1$ in Eq. (2), $\Delta H_{\text{disor.network,specific}}$ (max.) can be estimated to be 95 J/g.

## 3. Results

As discussed in the experimental part, three series of measurements (A)–(C) have been performed to evaluate $\Delta H_{\text{disor.network,specific}}$. They differ by the range of $T$ used and the technique. The first series (A) reports the data in a slow T-ramp between 30 and 140°C, the second (B) also in a slow T-ramp but between 5 and 98°C. The third gives the heat of immersion of amylose and glucose between 25 and 80°C. More data are obtained for (A) and (C) than for (B). The results are summarized in Table 1 where data found in the literature for starch have been added. Figs. 1–3 are typical traces obtained using techniques (A), (B) and (C) respectively.

(A) DSC in a slow T-ramp: $\Delta H_{\text{disor.network,specific}}$ between 30 and 140°C

Fig. 1a is a trace of dissolution at 1 K/h of a homogenized suspension of amylose. The integration of the heat flow between 30 and 140°C leads to $\Delta H_{\text{disor.network,specific}} = 60$ J/g with a maximum at 130°C. Fig. 1b is a baseline in the same conditions with water in the two cells. In other runs, with the same conditions, the values of $\Delta H_{\text{disor.network,specific}}$ show a spread of about 5%. The shape may vary from one experiment to another, the maximum being shifted or less pronounced than in Fig. 1a.Table 1 gives the averaged values of $\Delta H_{\text{disor.network,specific}}$ at three rates of heating (1, 3 and 6 K/h). The values of $\Delta H_{\text{disor.network,specific}}$, and consequently of $F$, are seen to decrease drastically when the rate of temperature scan increases. At 3 and 6 K/h, disordering is not complete as indicated by the low values of $\Delta H_{\text{disor.network,specific}}$, respectively, 26 and 12 J/g.

(B) DSC in a slow T-ramp: $\Delta H_{\text{disor.network,specific}}$ between 5 and 98°C.

Fig. 2 gives a typical trace obtained at 3 K/h with the Hart calorimeter and Table 1 the results. However, one sees by inspection of Fig. 1a that only a fraction of $\Delta H_{\text{disor.network,specific}}$ is evolved below 98°C. So one can expect that the values of $\Delta H_{\text{disor.network,specific}}$ obtained by the Hart calorimeter technique will be not complete. The values decrease rapidly when the rate of the T-ramp increases. The values are, as expected, much lower than those obtained in the C80 experiments, because part of the endotherm evolves at $T$ higher than 100°C.However, these experiments show clearly that an endotherm of dissolution exists in this non-crystalline amylose. The high sensitivity of the Hart calorimeter permits one to see details of the trace which are barely noticeable at the same temperature in Fig. 1a. The values of $\Delta H_{\text{disor.network,specific}}$, are rather scattered. This is due to the ambiguity of placing the

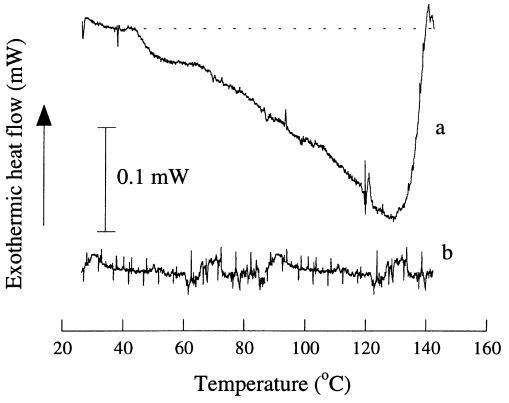


Fig. 1. (a) Typical trace of dissolution at 1 K/h between 40 and 140°C of a homogenized suspension of non-crystalline amylose. (b) Trace of a baseline in the same conditions.

[2] The result on the cohesion of polyolefin networks challenges the conventional view that the cohesive energy of a non-crystalline phase is that of a liquid and does not change much with temperature. However, since the existence of a network phase with high cohesion explains several obscure points in melts, gels and solutions it can be accepted as a fruitful model.

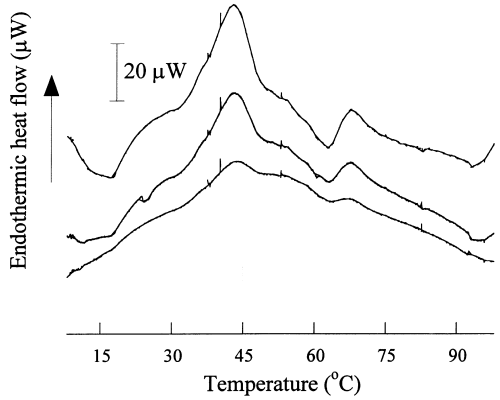


Fig. 2. Typical trace of dissolution at 3 K/h between 5 and 90°C of a homogenized suspension of non-crystalline amylose. The three traces correspond to different size aliquots of the same suspension placed in the three cells of the calorimeter and dissolved simultaneously.

base line when the T-ramp has to be interrupted in the middle of an endotherm, and due partly to the value of the signal/noise ratio which is not excellent for the low rate of heating with the Hart calorimeter.

(C) Isothermal heat of immersion: $\Delta H_{\text{disor.network,specific}}$ between 25 and 80°C, $\alpha_a$ at 25°C.

For glucose, the heat of immersion is endothermic and equal to 61.2 J/g. A typical trace of an isothermal heat of immersion of dried amylose is given in Fig. 3. To obtain $\Delta H_{\text{interaction,specific}}$, one has to subtract the heat of fusion of glucose found with the Perkin Elmer calorimeter: 180 J/g. Then, $\Delta H_{\text{interaction,specific}}$ is −118.8 J/g. For amylose the heat of immersion which is exothermic gives directly $\Delta H_{\text{interaction,specific}}$ since it is not crystalline. Its value is −57.2 J/g at 25°C as reported in Fig. 4 (Δ). Using Eq. (5), one finds $\alpha_a = 0.47$. Table 1, gives the value of $\alpha_a$ for a starch sample (Shiotsubo et al., 1986). It was calculated in the same way as for amylose (−17/−118.8 = 0.14).

The interaction of amorphous amylose with water is due to the formation of hydrogen bonds. The interaction

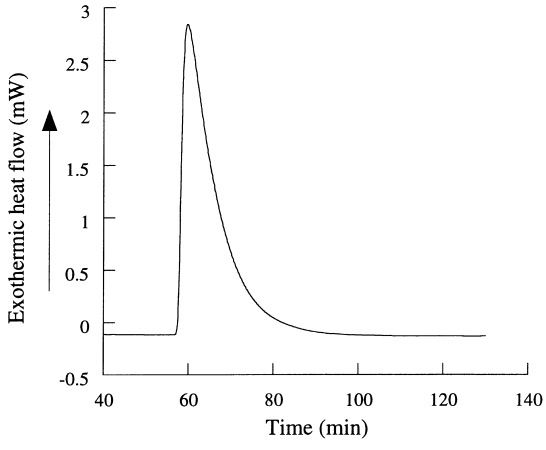


Fig. 3. Typical trace of an isothermal heat of immersion of dried amylose at 25°C. The heat effect lasts less than 100 min.

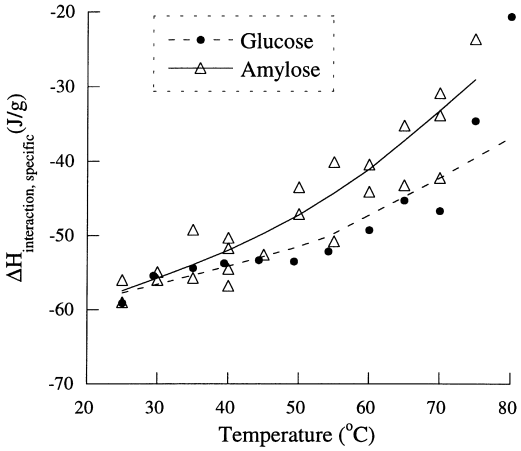


Fig. 4. Plot of $\Delta H_{\text{interaction,specific}}$ as a function of $T$ for amylose (△) and glucose (●). The difference between the two curves is $\Delta H_{\text{disor.network,specific}}$.

of a totally amorphous amylose with water is that of liquid glucose with water, namely −118.8 J/g or −22 kJ per ring of glucose (−118.8 J/g × 180 g/mol). This corresponds to the heat of formation of a hydrogen bond ($\Delta H_{\text{hbond}}$) multiplied by the number of bond per ring ($n_{\text{H2O}}$). $\Delta H_{\text{hbond}}$ is in fact the difference between amylose–water hydrogen bonds and that of water–water plus amylose–amylose ones. Molecular modeling and thermodynamics method leads to $n_{\text{H2O}} = 4$, (Fringant et al., 1995), and $\Delta H_{\text{hbond}} = -5.6$ kJ which is reasonable for the enthalpy of formation of a hydrogen bond.

### 3.1. $\Delta H_{\text{disor.network,specific}}(T)$

The experimental values of the heats of immersion are displaced towards less negative values as $T$ increases, as can be observed in Fig. 4 (upper curve). This is due to the weakening of the OH bonds in the aqueous solution as one approaches the boiling temperature of water. The heats of glucose and amylose do not change at the same rate however. In Table 2, the values of $\Delta H_{\text{interaction,specific}}$ are given at 25 and 80°C for three materials: glucose, amylose, and starch. The technique of Shiotsubo and Takahashi using a sensitive isothermal calorimeter is comparable to the present ones. The value of $\Delta H_{\text{interaction,specific}}$ at 25°C gives directly $\alpha_a = 0.14$ since the crystals of amylopectin are dissolved at that temperature. The difference $\Delta H_{\text{interaction,specific}}$ (80°C) − $\Delta H_{\text{interaction,specific}}$ (25°C) is given for amylose (33 J/g), starch (15 J/g) and glucose (44 J/g). When consideration is taken of the value of $\alpha_a$ for these three materials, the change of heat in the amorphous phase of these three compounds is widely different (69, 107, 44 J/g, respectively). Clearly for amylose and starch, another term, an endothermic part, contributes to the heat of immersion when $T$ increases. To obtain a quantitative value of $\Delta H_{\text{disor.network,specific}}$, between 25 and 80°C one has to use Eq. (8). On the lower curve of Fig. 4 are plotted the values of

Table 2
Values of $\Delta H_{\text{disor.network,specific}}$ by isothermal measurements

| | Setaram calorimeter (30–80°C) | | |
|---|---|---|---|
| | Glucose | Amylose | Starch[a] |
| $\Delta H_{\text{interaction}}$ (25°C) (J/g) | +61.2 | −57.2 | −17 |
| $\Delta H_{\text{interaction,specific}}$ (J/g) | −118.8 | −57.2 | −17 |
| $\Delta H_{\text{interaction}}$ (80°C)−$\Delta H_{\text{interaction}}$ (25°C) (J/g) | 44 | 33[b] | 15[c] |
| $\alpha_a$ (25°C) | 1 | 0.47 | 0.14[d] |
| $\Delta H_{\text{disor.network, specific}}$ (20–80°C) (J/g) | 0 | 12[e] | 9[f] |

[a] The long range order is not dissolved at 25°C.
[b] As read on Fig. 4.
[c] As obtained from Shiotsubo et al. (1984).
[d] See Eq. (5).
[e] $\Delta H_{\text{disor.network,specific}} = 33-\alpha_a \times 44 = 12$.
[f] $\Delta H_{\text{disor.network, specific}} = 15-\alpha_a \times 44 = 9$.

the second term of the right-hand side of Eq. (8). A constant value of $\alpha_a$ has been used in the temperature range to calculate this curve. The difference between the upper and lower curves is $\Delta H_{\text{disor.network,specific}}$. At 80°C the value is found to be about 12 J/g. This figure is consistent with the value obtained in Fig. 1 when the trace is integrated only between 30 and 80°C.

## 4. Discussion

### 4.1. $\Delta H_{\text{disor.network,specific}}$ between 40 and 140°C (A)

Amylose crystals with long-range order dissolve rapidly at equilibrium in water below 60°C (Shiotsubo et al., 1984; Shiotsubo et al., 1986). However, network amylose crystals dissolve with a $T_d$ spread across a large range between 50 and 140°C (this work). Other crystals of retrograded amylose dissolve in part between 75 and 165°C (Gidley et al., 1995; Sievert et al., 1989). Furthermore, the dissolution of short-range order depends critically on the rate of heating (Table 1). These features are unusual and have not been discussed in the literature. The concept of strain-dissolution which permits understanding of the characteristics of network dissolution will be presented now. References will be made on the fusion and dissolution traces of polyolefins by slow calorimetry because it is, on these systems, and by this technique, that phase-changes under strain have been investigated first.

### 4.2. Origin of strain

When a complex mixture is submitted to a T-ramp, the solvent and some of the polymeric material expands but strain develops in the network phase because of the junctions between chains which limit their expansion. The nature of the junctions (hydrogen bonds, entanglements, covalent bonds) is not important as long as the junctions are temperature stable. This strain generated in the network by the T-ramp could be qualified of internal strain. It has specific consequences on the melting process as seen below.

### 4.3. The solid–solution diagram (strain, $T_d$) under external and internal strain

The diagram (strain, $T_d$) of Fig. 5 illustrates the effect on the phase-change of different conditions of strain build-up.

In Fig. 5a the sample is simply submitted to an external strain, $S_{\text{external}}$, such as putting a constant tension on the material during dissolution. In the phase diagram which separates the solid from the solution, $T_d$ is seen to increase from $T_{d,0}$ to $T_{d,S}$. The temperature, $T_{d,S}$ corresponds to the point on the equilibrium line, (strain, $T_d$) between the solid and the solution (curve 1) associated with the value of

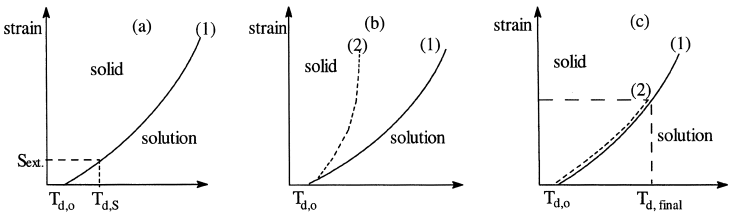


Fig. 5. Solid–solution as a function of strain. (a) An external strain is applied on a sample free of network; $T_d$ is raised from $T_{d,0}$ to $T_{d,S}$. (b) Development of internal strain in a fast T-ramp. Strain increases faster than the ($T$, strain) equilibrium line. At the end of the ramp, the material at ($T_{\text{final}}$, $S_{\text{final}}$) is still solid. (c) Development of internal strain in a slow T-ramp. Strain increases but along the equilibrium line. The material is partially or completely disordered.

$S_{external}$. The shape of the endotherm of dissolution showing the heat effect versus temperature has no reason to be different from that obtained without strain because the strain is kept constant during the T-ramp. Melting traces of fibres whose extremities have been tightened to the calorimetric cell indicate that $T_m$ is indeed higher for constrained chains than for free chains.

The same curve 1 can be used to delimit the regions of phase equilibrium for Fig. 5b,c which stand for the cases of dissolution under an internal strain. When the strain is generated by the process of dissolution itself, it does not have a fixed value but increases during the T-ramp. Its rate of increase depends on conditions of melting/dissolution.

In a fast T-ramp (Fig. 5b), the strain in the network increases so fast that the system cannot cross the boundary between the solid and the solution. The dotted line (2) in Fig. 5b represents a fast increase of strain is not a solid–liquid equilibrium line. These conditions prevail in the usual fast T-ramp (600 K/h). The value of $\Delta H_{disor.network,specific}$ is zero or low because the solid state is the equilibrium state in the conditions of a fast ramp. The dissolution of short range order has been missed because a technique suited to non-strainable long-range order has been systematically applied to polymers whose non-crystalline phase is responsive to deformation.

In a slow-ramp (Fig. 5c), on the other hand, the strain in the network (dotted line (2)) increases slowly along the equilibrium line (1). Several situations can occur: dissolution occurs continuously and is complete; dissolution can be observed then be arrested when strain increases faster with $T$ than curve 1 and be not complete; dissolution can resume after arrested dissolution took place over a variable T-ramp and be ultimately complete. Conditions of dissolution lead to either complete or partial dissolution of the network.[3]

### 4.4. Typical trace of dissolution in a slow T-ramp

Fig. 6 shows two examples of schematic traces of dissolution in a slow T-ramp. In Fig. 6a, the polymer possesses long-range order but not in Fig. 6b. The peak with a large heat flow at $T_d$ corresponds to the dissolution of long-range order. The flat endotherms below and above $T_d$ are the dissolution of the network. These flat endotherms are a unique feature of slow DSC. The range of temperature of the phase change is controlled by strain. Strain build-up and occasionally strain-release in the network depend on the

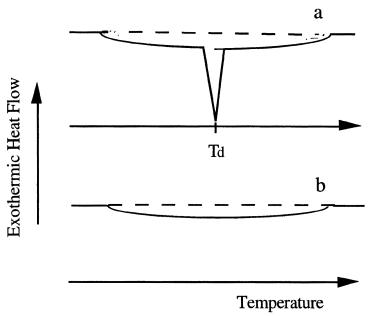


Fig. 6. Schematic traces of dissolution in a slow T-ramp. (a) Semi-crystalline sample: endotherms of dissolution of long-range order (with a peak at $T_d$), and short-range order. (b) Non-crystalline sample: endotherm of dissolution of the short-range order. $T_{d,final}$ is a near-equilibrium dissolution temperature. The other temperatures along $T_{d,final}$ are not.

conditions of the dissolution. As a consequence, the limits in temperature of the flat endotherms are sensitive to small differences in the conditions of dissolution. This feature does not exist for the main endotherm. The value of $T_d$ for the non-strained long-range order crystals diminishes by only a few kelvin when the rate of heating is reduced (Shiotsubo et al., 1984). Characterization of the flat endotherms requires special conditions, i.e. conditions which minimize the strain.

The term dissolution is used in a broad sense. The end of the flat endotherm in Fig. 6 does not signify that the mixture is a real solution but that there is no more meltable order in the conditions of the system (temperature, strain, concentration, number of heating/cooling cycles).

For polyolefins, the phase-changes whose heat effects are shown in Fig. 6 are reversible. When the temperature is lowered slowly, traces which are the mirror-image of those in Fig. 6 are obtained.

### 4.5. Case of amylose

The endotherm of Fig. 1a is rather flat and extends from $T_{d,0}$ to $T_{d,final}$, this last temperature being related to $S_{int,fin}$. The traces obtained at 3 and 6 K/h with amylose are intermediate cases between those illustrated in Fig. 5b and c. The values of $\Delta H_{disor.network,specific}$ are small because at the end of the experiment a fraction of network crystals are in the solid phase region of the (strain, $T$) diagram. The correlation between the rapidity of the T-ramp on the build-up of strain is reasonable. A fast T-ramp does not leave enough time for the chains to disentangle and avoid high strain.

In the process of disordering a network, complex phenomena occur. Some molecules escape the network, others are still bonded by knots or entanglements or strained crystals. The final concentrations of the different morphologies depend on the history of the sample including some features which are difficult to control. Another effect can accompany the disordering of the chains and the building up of strain in the T-ramp. A sudden increase of strain displaces the representative point in the (strain, $T$) diagram

[3] According to classical thermodynamics, the effect of pressure ($P$) and of strain ($S$) on the two phases in equilibrium (solid and liquid (or dissolved)) depends on the volume $V$ of the phase through the relation $\partial G/\partial S \simeq \partial G/\partial P = V$. The displacement of $T_d$ or $T_m$ depends on the relative effect of the strain on the two phases in equilibrium. In most systems $V_{liquid} > V_{solid}$ so that $T_d$ or $T_m$ increases with $P$ or $S$. Because of the complex interactions between the phases of amorphous amylose and water, an exact prediction of d$G$/d$S$ is not possible. However, the trend shown in Fig. 5 is qualitatively correct and can be used as a phenomenological correlation which brings better understanding of the complex amylose mixtures as it did for the polyolefins solutions and gels.

towards the solid phase. It corresponds to the recrystallization of the amylose chains during the ramp which leads to an exothermic spike on the trace. This effect is similar to the phenomena which appears as a whitening effect when a PE film is stretched by hand or is put in a solvent at a temperature below $T_d$. In samples which have not been homogenized by stirring, prior to the T-ramp, excess of strain and local high amylose concentration lead to such exothermic peaks.

The two following traces obtained in a 6 K/h T-ramp are examples of recrystallization during the ramp. In Fig. 7a ($c = 1.5\%$), dissolution and recrystallization occur consecutively in the T-ramp and $\Delta H_{\text{disor.network,specific}}$ is about 24 J/g. In Fig. 7b ($c = 10\%$) a large peak of recrystallization occurs at 130°C and $\Delta H_{\text{disor.network,specific}}$ is only 12 J/g.

In a region of arrested melting/dissolution, the increase of strain is too small to lead to recrystallization but large enough to prevent further fusion/dissolution.

### 4.6. Network fraction and resistance to chain scission

Native amylose is resistant to enzyme degradation and it is only after a heat treatment in the presence of water that susceptibility to enzyme attack develops. The susceptibility

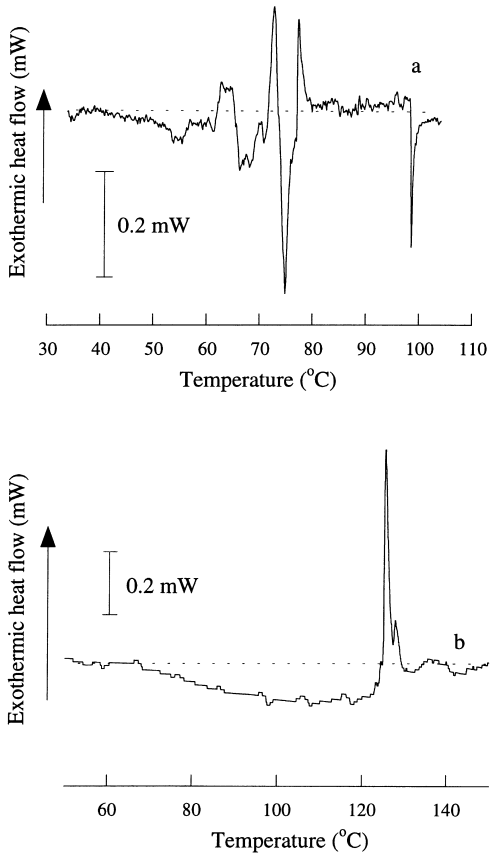


Fig. 7. Typical traces of dissolution of non-homogenized suspension of amylose showing recrystallization peaks and partial dissolution. (a) $c = 1.5\%$ $v = 6$ K/h $\Delta H_{\text{disor.network,specific}} = 24$ J/g. (b) $c = 10\%$ $v = 6$ K/h $\Delta H_{\text{disor.network,specific}} = 12$ J/g.

is such that degradation is not always complete, since a fraction of amylose after retrogradation stays resistant or develops a resistance to amylolyse. As remarked upon by several authors (Gidley et al., 1995) in their investigation of the resistant fraction, there is no clear link between the observed resistance and either the magnitude of X-ray crystallinity, or the crystalline modification of the long-range order. Since the amorphous phase is not likely to confer a special resistance to amylolyse, one can hypothesize that the network phase is responsible for the resistance and that any change in its morphology alters the response of the material to amylase.

In a native sample, the different phases are linked by the network phase which is spread evenly throughout the sample. This homogeneity and the high cohesive energy of the network phase (as revealed by the high value of $\Delta H_{\text{disor.network,specific}}$ found above) are important factors in the resistance to amylolyse. During heating, macroscopic and microscopic changes take place: the appearance of the mixture indicates that the network has been fragmented and distributed in the solvent. The calorimetric trace shows that it has been disordered. On cooling, long-range and short-range orders grow, the amount of each depending on the solution's thermal history. Dissolution and recrystallization are not, however, equilibrium phase-changes which cancel each other. The native morphology has been changed irreversibly by the treatment. The domains associated with the different phases are now larger and more separate. As a consequence, long-range order growth is eased, as the impediment to growth that were the network chains is removed. It was shown recently that a high autoclave temperature (170°C) produces, on cooling, a material having a sharper X-ray diagram (Doublier et al., 1992) than when the autoclave temperature is lower. The network phase which permits gel formation is still present but it is weaker due to modification in the distribution of junctions. The fragmentation of the network makes the retrograded amylose more responsive to amylolyse than is the native amylose. The hypothesis of irreversible change in the network at high temperature is supported by recent work (Keetels et al., 1996). They found that gels left at 120°C when aged at room temperature did not recover their original value of Young's modulus.

The separation of the phases which occurs for polyolefins during fusion/crystallization is illustrated by their $^{13}C$ NMR spectra. The spectrum of nascent PE has a single peak whereas that of the melted and recrystallized sample has two peaks, corresponding to the orthorhombic and amorphous morphologies (Morin et al., 1995). The presence of the amorphous peak in the recrystallized sample and its absence in the nascent is surprising. Since the X-ray and density crystallinities of the recrystallized sample are higher than that of the nascent sample, one would expect the amorphous peak to be less important in the recrystallized sample.

The enzyme-resistant fraction of amylose can be a residue of the native network or a result of the treatment. The wide

range of percentages of enzyme resistant amylose reported in the literature (5–70%) reflects the important role of the kinetics parameters in the stability or growth of this phase.

### 4.7. Network fraction in polyolefins

One of the treatments applied to amylose solutions to increase the enzyme-resistant fraction has been to submit them to a succession of cycles of heating and cooling (Biliaderis, 1991; Sievert et al., 1989). In the same way, cycles of temperature have been made in the calorimeter on polyolefins and polyolefin solutions (Phuong-Nguyen et al., 1992a, b) to modify the network content. This change was measured through melting and dissolution traces similar to Fig. 6. In the absence of solvent, the network phase increases from 30 to 50% between the first and second cycles (done at 1 K/h). In dilute solutions (1%), on the other hand, a large number of cycles i.e. 10–12, has the effect of diminishing the network fraction and its strain (Phuong-Nguyen et al., 1992b; Delmas, 1993). It was found that slow crystallization of the dilute solution was important in the disentanglement process. For the high molecular weight samples investigated, the network tension was loosened and its concentration diminished. The concentration of the amylose mixtures is sufficiently high to make them behave more like melts of polyolefins than dilute solutions so that the network fractions are increased in the cycles. During the residence time at high temperature more entanglements are formed. They are frozen in a fast-cooling process which leads to an increase of the network phase. It is thought that cycles of low and high temperatures favor separation of the phases to an extent which depends on the rate of cooling.

### 4.8. High-temperature endotherm in amylase-resistant amylose

High-temperature endotherms (130–165°C) have been observed on the dissolution traces of amylose/water mixtures which have undergone a high-temperature treatment followed by cooling (Appelqvist et al., 1993; Sievert et al., 1993b, 1989). The integration of the heat flow over a large $T$ interval leads to enthalpy of disordering whose maximum value is around 20–25 J/g (5–10 K/min). The enthalpies vary as expected with the origin of amylose and the history of the solution. On non-retrograded samples, the enthalpies are less than 8 J/g.

Remembering the correlation described above between the rate of heating and the meltable enthalpy, one wonders why sizable high-temperature endotherms could be observed in a rapid T-ramp while they cannot be seen on the nascent sample. The answer seems to be that heat treatment decreases the number of junctions in the retrograded amylose and hence strain build-up in the network. Non-equilibrium dissolution can then take place in a faster T-ramp below the temperature of amylose degradation. Furthermore, fast DSC very likely leads to an incomplete disordering if the enthalpy found with the 1 K/h T-ramp (60 J/g) can be taken as an indication of complete or semi-complete dissolution.

Finally, high sensitivity of the endotherm characteristics to the sample history is a marker of strain dissolution. The strain acquired by the system during the T-ramp is influenced by small differences in parameters which are difficult to control exactly. These markers are the following: homogeneity of the suspension, thermal history (autoclaving temperature, rate of heating, etc.), deformation of the gel, method of drying, temperature gradient inside the sample. It is therefore no surprise that reproducible results are difficult to obtain in the preparation and characterization of the fraction of enzyme-resistant amylose or starch.

### 4.9. Comparison with solid state $^{13}C$ NMR characterization

$^{13}C$ NMR analysis has been used extensively to probe the organization of polysaccharides such as cellulose, starch and amylose (Neregin et al., 1986; Gidley and Bociek, 1985; Colquhoun et al., 1995). The soluble amylose spectra have permitted the allocation of the resonance lines to the different carbon atoms in the repeating unit. The preparation of samples with different modifications and different crystallinity permits an association of the details of the resonance lines with the crystalline modifications and also with the presence of amorphous amylose. Composite spectra of crystalline and amorphous amylose can be made to match an experimental result and evaluate the crystalline fraction $\alpha_c$ (NMR) of a given sample. Several points can be made concerning the correlation of the evaluation of order by slow calorimetry and by $^{13}C$ NMR.

1. The quantitative evaluation of the two phases of amorphous amylose made from the heats of swelling has no equivalent in the $^{13}C$ NMR analysis where the network phase is included in the amorphous phase. However, the spectrum of amorphous amylose is reported (Gidley and Bociek, 1985) to correspond to the overlapping of spectra with narrow and large chemical shift ranges. Comparison of the spectra and heats of swelling of different amorphous amyloses could allow a separation of the amorphous amylose spectrum into contributions due to the network phase and of the totally disordered parts of amorphous amylose. Advances in the understanding of the (NMR) spectrum of the network phase could be made by taking the spectra of amorphous amyloses with different fractions of network phase as measured by heats of swelling. By extrapolation, the spectrum of a network free amylose could be obtained.
2. Calorimetry permits one to follow events in the polymer/solvent system but the molecular origin of these has to be suggested by a model or revealed by other techniques. Also specific information on the nature of the stable junctions of the network (entanglements, small crystal-

lites, stable associations strainable in a T-ramp) must be looked for using molecular techniques. The model presented by NMR (Gidley and Bociek, 1985) of isolated double helices is very relevant to the network formation. If a given amylose molecule has a partner, not itself but another amylose molecule in the double-helices segments, a very stable network is formed. The junctions may be bundles of double helices or isolated double helices. The effect of temperature is to separate the bundles, loosen the double helices, and free some molecules as simple helices or random coils in the solvent. These events may follow or more likely overlap in the time/temperature framework of the dissolution. The difference of enthalpy of disordering between the NMR and calorimetry experiment (10 J/g) (Cooke et al., 1992) and the slow calorimetry experiment (60 J/g) indicates that the disordering is more complete in the slow experiment. The difference in temperature range points out to a counter-intuitive observation namely that the molecular order is more resistant to heat than crystalline order. This is a consequence of its insertion into a network. It would be very informative to make a ''slow NMR experiment''. The change of spectra with temperature could possibly be interpreted as stages of disordering in which the bundles disappear and the transformation of double helices into singles helices and random coils take place. As long as the network has some cohesion, one would expect the transition not to be cooperative. The spectrum obtained at the end of the experiment when no more meltable is left, would be useful for quantitative analysis of the spectra taken before and after $T_d$.

3. The molecular order in the $^{13}C$ NMR analysis is associated with double helix conformations which are present in the crystalline and amorphous phases. Is the disordering observed by slow calorimetry equivalent to the change of double to single helix conformation or is there a more complete process which transform the helices into random coils? The molecular weight dependence of the intrinsic viscosity of dilute solutions of amylose are consistent with a random coil conformation. The value of $\Delta H_{total}$ (60 J/g) is much larger than the fraction of the heat evolved during gelatinisation which corresponds to the destruction of molecular order (about 10 J/g for a total enthalpy of gelatinisation of 16 J/g). This points clearly to a large fraction of molecular order left in the system after gelatinization. Based on the NMR result that double helices disappear above $T_d$, the enthalpy found must correspond to the transformation of single helices into random coils. However, it seems unlikely that just after the disappearance of long-range order the double helix content has vanished as it seems also unlikely that the amorphous amylose does not contain a fraction of double helices. The supposition of total disappearance of the double helices is the basis of the NMR analysis. It is possible that the double helix–single helix transition is not a cooperative phenomena. The presence of short segments of double helices either in the amorphous amylose or the amylose treated at $T_d$ presents its detection in $^{13}C$ NMR.

## 5. Conclusion

In the present paper, we have presented the phenomenon of strain dissolution. First found in polyolefin solutions, it seems to be a general occurrence in materials where the chains can form a physical network. In a strain situation, phase-change is prevented, i.e. dissolution is delayed. The origin of the strain is the inability of the network chains to be in equilibrium with the sudden expansion imposed on the system by fast T-ramps.

We suggest that a physical network is responsible for the resistance to amylolyse of retrograded amylose. The amount of physical network depends on the solution treatment. The conditions which increase the fraction of enzyme-resistant amylose are similar to those used to control the network phase of polyolefins.

A physical network is also responsible for the resistance to amylolyse of native amylose but it is different from that of retrograded amylose. It is homogeneously distributed throughout the sample and has an order which is not meltable under the usual conditions of fast DSC. By using slow calorimetry (typically a ramp of 1 K/h), the conditions to reduce the strain building in the network are met in a manner revealed by the enthalpy of disordering the network of native amylose. Its value (60 J/g) is high compared to those reported by fast DSC. The comparison of this enthalpy with the enthalpy of melting glucose crystals suggests that disordering of the native network is not complete under the conditions used.

By finding the conditions to melt the short-range order or the molecular order, the present results make a bridge between calorimetric and spectroscopic data and suggest strategies to use $^{13}C$ NMR in order to observe directly the dissolution of molecular order.

The literature reports difficulty in collecting reproducible data (range of $T_d$, enthalpy of dissolution) of complex systems such as amylase-resistant amylose or other gel-forming polymers. This feature, by itself, could be considered as a tracer of the presence of a strainable network. It has its origin in the combined sensitivity of the phase-change temperature to strain and the actual strain itself to the sample history.

The stability of the Setaram calorimeter in slow T-ramp permits accurate measurements of heats evolved over a large interval of temperature.

Heats of immersion measurements of dried amylose between 25 and 80°C permit us to evaluate the amorphous content of native amylose and to observe the beginning of the network disordering below 80°C.

## Acknowledgements

The financial support of the NSERC of Canada is gratefully acknowledged. We thank our colleague Dr. M. A. Mateescu for interesting us with the physico-chemical properties of amylose and Dr C. Gicquaud of the Université du Québec à Trois-Rivières for the measurements taken with the Hart calorimeter.

## References

Appelqvist, I. A. M., Cooke, D., Gidley, M. J., & Lane, S. J. (1993). *Carbohydrate Polymers*, *20*, 291–299.

Banks, W., & Greenwood, C. T. (1975). *Starch and its components*. Edinburgh: Edinburgh University Press.

Biliaderis, C. G. (1991). In H. Levine & L. Slade (Eds.), *Water relationship in food* (pp. 251–273). New York: Plenum Press.

Clark, A. H., & Gidley, M. J. (1989). *Macromolecules*, *227*, 346–351.

Colquhoun, I. J., Parker, R., Ring, S. G., Sun, L., & Tang, H. R. (1995). *Carbohydr. Polym.*, *27*, 255–259.

Cooke, D., & Gidley, M. J. (1992). *Carbohydr. Res.*, *22*, 105–112.

Delmas, G. (1993). *J. Polym. Sci., Polym. Phys. Ed.*, *31*, 2011–2018.

Dev, S. B., Burum, D. P., & Rha, C. K. (1987). *Spectrosc. Lett.* , *29*, 853–869.

Doublier, J. L., Cole, I., Hamas, G., & Charlet, G. (1992). *Prog. Colloid Polym. Sci.* , *90*, 1–5.

Durrani, C. M., & Donald, A. M. (1995). *Polym. Gels Networks*, *3*, 1–27.

Fringant, C., Tvaroska, I., Mazeau, K., Rinaudo, M., & Desbrieres, J. (1995). *Carbohydr. Res.*, *278*, 27–41.

Gidley, M. J., & Bociek, S. M. (1985). *J. Am. Chem. Soc.*, *107*, 7040–7044.

Gidley, M. J., Cooke, D., Darke, A. H., Hoffmann, R. A., Russel, A. L., & Greenwell, P. (1995). *Carbohydr. Polym.* , *28*, 23–31.

Hollinger, G., Kuviak, L., & Marchessault, R. H. (1974). *Biopolymers*, *13*, 879–890.

Jasra, R. V., & Ahluwalia, J. C. (1982). *J. Sol. Chem.* , *11*, 325–338.

Keetels, C. J. A. M., Van Viet, T., & Walstra, P. (1996). *Food Hydrocolloids*, *10*, 363–368.

Miles, J. J., Morris, V. J., & Rings, S. G. (1985). *Carbohydr. Res.*, *235*, 257–269.

Miles, J. J., Morris, V. J., Orford, P. D., & Ring, S. G. (1985). *Carbohydr. Res.*, *135*, 271–281.

Morin, F., Delmas, G., & Gilson, D. (1995). *Macromolecules*, *28*, 3248.

Neregin, P. P., Fyfe, C. A., Marchessault, R. H., & Taylor, M. G. (1986). *Macromolecules*, *19*, 1030–1034.

Noël, T. R., & Ring, S. G. (1992). *Carbohydr. Res.*, *227*, 203–213.

Phuong-Nguyen, H., & Delmas, G. (1992). *Macromolecules*, *25*, 414–421.

Phuong-Nguyen, H., & Delmas, G. (1992). *Macromolecules*, *25*, 408–414.

Phuong-Nguyen, H., & Delmas, G. (1994). *J. Mater. Sci.*, *29*, 3612–3620.

Phuong-Nguyen, H., & Delmas, G. (1994). *Thermochim. Acta*, *238*, 257.

Phuong-Nguyen, H., & Delmas, G. (1994). *J. Sol. Chem.*, *23*, 249–261.

Phuong-Nguyen, H., & Delmas, G. (1995). *Collect. Czech. Commun*, *60*, 1905–1924.

Shiotsubo, T., & Takahashi, K. (1984). *Agric. Biol. Chem.*, *48*, 9–17.

Shiotsubo, T., & Takahashi, K. (1986). *Carbohydr. Res.*, *158*, 1–6.

Sievert, D., & Pomeranz, Y. (1989). *Cereal Chem.*, *66*, 342–347.

Sievert, D., & Würsch, P. (1993). *Cereal Chem.*, *70*, 333–338.

Sievert, D., & Wursch, P. (1993). *J. Food Sci.*, *58*, 1332–1335.

Strauss, U. P., Porcja, R. J., & Chen, S. Y. (1990). *Macromolecules*, *23*, 172–175.

Welsh, E. J., Bailey, J., Chandarana, R., & Noris, W. E. (1992). *Prog. Food Nutr. Sci.*, *6*, 45–53.